

XMRVの疫学に関する主な文献一覧

文献番号	文献名	XMRVの陽性率			検出法(組織)	報告国	要約
		前立腺がん	慢性疲労症候群	健康人			
1	Urisman A, et al., PLoS Pathog. 2006 Mar;2(3):e25. Identification of a novel Gammaretrovirus in prostate tumors of patients homozygous for R462Q RNASEL variant.	9/86 10.5% (遺伝子の型による内訳) QQ 8/20 40% RQ 0/14 0% RR 1/52 1.9%			RT-PCR (前立腺)	米国	DNAアレイによって前立腺がん組織から新たなウイルス(XMRV)を発見した。RNaseLにホモ型変異(QQ)にもつ前立腺癌の40%からXMRVが検出されたが、変異がない前立腺癌(RR)では1.9%であった。
2	Fischer N, Hellwinkel O, Schulz C, Chun FK, Huland H, Aepfelbacher M, Schlomm T. J Clin Virol. 2008 Nov;43(3):277-83 Prevalence of human gammaretrovirus XMRV in sporadic prostate cancer	1/87 1.2% (非家族性)		1/70 1.42%	RT-PCR (前立腺)	ドイツ	非家族性の前立腺がん組織からXMRVの検出が試みられた。その結果、欧州北部においてはほとんど検出されなかった。但し、本研究において、RNaseLにホモ型変異(QQ)をもつサンプルは6%未満であったことに注意を要する。
3	Hohn O, Krause H, Barbarotto P, Niederstadt L, Beimforde N, Denner J, Müller K, Kurth R, Bannert N. Retrovirology. 2009 Oct 16;6:92. Lack of evidence for xenotropic murine leukemia virus-related virus(XMRV) in German prostate cancer patients	0/589 0% (PCR) 0/146 0% (抗体)		0/5 0% (抗体)	PCR, RT-PCR (前立腺) ELISA(血清)	ドイツ	589例(76例の RNaseLホモ型変異(QQ)を含む)の前立腺がん組織からDNAとRNAを抽出し、核酸増幅法を用いてXMRVの遺伝子の有無を調べたが検出できなかった。また、血清中からもXMRVに反応する抗体は検出できなかった。
4	Schlaberg R, Choe DJ, Brown KR, Thaker HM, Singh IR. Proc Natl Acad Sci U S A. 2009 Sep 22;106(38):16351-6 XMRV is present in malignant prostatic epithelium and is associated with prostate cancer, especially high-grade tumors	14/233 6.2% PCR 54/233 23% ウイルス抗原		2/101 2% PCR 4/101 4% ウイルス抗原	PCR (前立腺) 組織染色 (前立腺)	米国	233例の前立腺癌中14例からPCR法によってXMRV遺伝子が検出された。RNaseLの変異とは関連がなかった。XMRVのタンパクは上皮細胞に存在していた。
5	Lombardi VC, Ruscetti FW, Das Gupta J, Pfost MA, Hagen KS, Peterson DL, Ruscetti SK, Bagni RK, Petrow-Sadowski C, Gold B, Dean M, Silverman RH, Mikovits JA. Science. 2009 Oct 23;326(5952):585-9 Detection of an infectious retrovirus, XMRV, in blood cells of patients with chronic fatigue syndrome		68/101 67%	8/218 3.7%	PCR (末梢単核球)	米国	慢性疲労症候群(CFS)患者の67%からXMRV遺伝子が検出され、XMRVに感染したCFS患者の細胞や血液中に感染性ウイルスが存在した。また、一部の症例ではウイルスと抗体が共存していた。健康人の3.7%からもXMRVが検出された。CFS由来のXMRVは塩基配列が前立腺癌由来のものと同様を形成していた。
6	Erwein O, Kaye S, McClure MO, Weber J, Willis G, Collier D, Wessely S, Cleare A. PLoS One. 2010 Jan 6;5(1):e8519. Failure to detect the novel retrovirus XMRV in chronic fatigue syndrome		0/186 0%		PCR (全血)	イギリス	慢性疲労症候群186例を対象に全血から核酸増幅法によるXMRV遺伝子の検出を行ったが、検出できなかった。
7	Groom HC, Boucherit VC, Makinson K, Randal E, Baptista S, Hagan S, Gow JW, Mattes FM, Breuer J, Kerr JR, Stoye JP, Bishop KN. Retrovirology. 2010 Feb 15;7:10 Absence of xenotropic murine leukaemia virus-related virus in UK patients with chronic fatigue syndrome		0/136 0% DNA 0/140 0% RNA	0/95 0% DNA 0/141 0% RNA	PCR(全血) RT-PCR(血清)	イギリス	全血及び血清から核酸を抽出し、核酸増幅法を用いてXMRVの遺伝子を検出したが、慢性疲労症候群及び健康人から検出されなかった。
8	van Kuppeveld FJ, de Jong AS, Lanke KH, Verhaegh GW, Melchers WJ, Swanink CM, Bleijenberg G, Netea MG, Galama JM, van der Meer JW. BMJ. 2010 Feb 25;340:c1018 Prevalence of xenotropic murine leukaemia virus-related virus in patients with chronic fatigue syndrome in the Netherlands: retrospective analysis of samples from an established cohort		0/32 0% RNA	0/43 0% RNA	RT-PCR (末梢単核球)	オランダ	1991~1992年に凍結保存されていた末梢単核球からRNAを抽出し、核酸増幅法によってXMRV遺伝子を検出したが、慢性疲労症候群及び健康人から1例も検出されなかった。

OPEN ACCESS Freely available online
PLOS PATHOGENS

Identification of a Novel Gammaretrovirus in Prostate Tumors of Patients Homozygous for R462Q RNASEL Variant

Anatoly Urisman^{1*}, Ross J. Molinaro^{2,3*}, Nicole Fischer^{4*}, Sarah J. Plummer⁵, Graham Casey², Eric A. Klein³, Krishnamurthy Malathi⁶, Cristina Magi-Galluzzi⁷, Raymond R. Tubbs⁸, Don Gamm^{9,7a}, Robert H. Silverman^{3*}, Joseph L. Delfino^{1,8*}

1 Department of Biochemistry and Biophysics, University of California San Francisco, San Francisco, California, United States of America, **2** Department of Cancer Biology, Lerner Research Institute, Cleveland Clinic, Cleveland, Ohio, United States of America, **3** Department of Chemistry, Cleveland State University, Cleveland, Ohio, United States of America, **4** Department of Microbiology and Immunology, University of California, San Francisco, California, United States of America, **5** Gillman Urological Institute, Cleveland Clinic, Cleveland, Ohio, United States of America, **6** Anatomic and Clinical Pathology, Cleveland Clinic, Cleveland, Ohio, United States of America, **7** Department of Medicine, University of California, San Francisco, California, United States of America, **8** Howard Hughes Medical Institute, University of California San Francisco, San Francisco, California, United States of America

Ribonuclease L (RNase L) is an important effector of the innate antiviral response. Mutations or variants that impair function of RNase L, particularly R462Q, have been proposed as susceptibility factors for prostate cancer. Given the role of this gene in viral defense, we sought to explore the possibility that a viral infection might contribute to prostate cancer in individuals harboring the R462Q variant. A viral detection DNA microarray composed of oligonucleotides corresponding to the most conserved sequences of all known viruses identified the presence of gammaretroviral sequences in cDNA samples from seven of 11 R462Q-homozygous (QQ) cases, and in one of eight heterozygous (RQ) and homozygous wild-type (RR) cases. An expanded survey of 86 tumors by specific RT-PCR detected the virus in eight of 20 QQ cases (40%), compared with only one sample (1.5%) among 66 RQ and RR cases. The full-length viral genome was cloned and sequenced independently from three positive QQ cases. The virus, named XMRV, is closely related to xenotropic murine leukemia viruses (MuLV), but its sequence is clearly distinct from all known members of this group. Comparison of gag and pol sequences from different tumor isolates suggested independent infection with the same virus in all cases, yet sequence variation was consistent with the infection being independently acquired. Analysis of prostate tissues from XMRV-positive cases by *in situ* hybridization and immunohistochemistry showed that XMRV nucleic acid and protein can be detected in about 1% of stromal cells, predominantly fibroblasts and hematopoietic elements in regions adjacent to the carcinoma. These data provide to our knowledge the first demonstration that xenotropic MuLV-related viruses can produce an authentic human infection, and strongly implicate RNase L activity in the prevention or clearance of infection *in vivo*. These findings also raise questions about the possible relationship between exogenous infection and cancer development in genetically susceptible individuals.

Citation: Urisman A, Molinaro RJ, Fischer N, Plummer SJ, Casey G, et al. (2006) Identification of a novel gammaretrovirus in prostate tumors of patients homozygous for R462Q RNASEL variant. PLoS Pathog 2(3): e25.

Introduction

Type I Interferons (IFNs) are rapidly mobilized in response to viral infection and trigger potent antiviral responses. One such response is the induction by IFN of a family of 2'5' oligoadenylate synthetases (OAS); upon activation by virally encoded dsRNA, these enzymes produce 5'-phosphorylated 2'5' linked oligoadenylates (2-5A) from ATP [1]. 2-5A, in turn, is an activator of ribonuclease L (RNase L) [2], which degrades viral (and cellular) single stranded RNAs [3]. *In vivo* evidence for the antiviral role of the 2-5A system was provided by studies with RNase L^{-/-} mice, which have enhanced susceptibility to infections by the picornaviruses, encephalomyocarditis virus, and Coxsackievirus B4 [4,5]. Ultimately, sustained activation of RNase L triggers a mitochondrial pathway of apoptosis that eliminates virus-infected cells [4,6-8]. Genetic lesions in RNase L impart this apoptotic response, which has raised interest in the possibility that such mutations might also contribute to malignancy [9].

* PLoS Pathogens | www.plospathogens.org

0211

March 2006 | Volume 2 | Issue 3 | e25

Editor: Susan Ross, University of Pennsylvania School of Medicine, United States of America
Received November 29, 2005; Accepted February 23, 2006; Published March 31, 2006
DOI: 10.1371/journal.ppat.0020025
Copyright: © 2006 Urisman et al. This is an open-access article distributed under the terms of the Creative Commons Attribution License, which permits unrestricted use, distribution, and reproduction in any medium, provided the original author and source are credited.
Abbreviations: 2-5A, 5'-phosphorylated 2'5' oligoadenylate; aa, amino acid; FISH, fluorescence *in situ* hybridization; Hg, hematoxylin; and mouse hCG, heterodimeric prostate cancer; IFN, interferon; IHC, immunohistochemistry; RT, long terminal repeat; MCF, milk cell foci-inducing murine leukemia virus; MTRC, murine type C retrovirus; MuLV, murine leukemia virus; n, nucleotide; NZB-9-1, New Zealand Black 9-1 xenotropic retrovirus; ORF, open reading frame; PBS, phosphate-buffered saline; PCR, polymerase chain reaction; QO, RNASEL homozygous; RQ, RNASEL heterozygous; RNase L, Ribonuclease L; RR, RNASEL wild-type; RT-PCR, reverse transcription polymerase chain reaction; XMRV, xenotropic murine leukemia virus-related virus; XN, xenotropic and polytropic retrovirus receptor.
* To whom correspondence should be addressed. E-mail: joe@dentlab.ucsf.edu (JLD), silverm@ccf.org (RHS)
© These authors contributed equally to this work.

viral sequences, by hybridization to a DNA microarray composed of the most conserved sequences of all known human, animal, plant, and bacterial viruses [20,21]. Here we report that 40% (eight of 20) of all tumors homozygous for the R462Q allele harbored the genome of a distinct gammaretrovirus closely related to xenotropic murine leukemia viruses (MuLVs). In contrast, retroviral sequences were present in <2% of tumors bearing at least one copy of the wild-type allele (one of 66). In addition, virus-harboring cells were detected within infected prostatic tumor tissues by fluorescence in situ hybridization (FISH) and immunohistochemistry (IHC). These findings represent the first detection of xenotropic MuLV-like agents in humans, and reveal a strong association between infection with the virus and defects in RNase L activity. The relation of retroviral infection to prostate cancer will require further study, but a cofactor role is not excluded.

Results

Detection of XMRV by Microarray-Based Screening

To search for potential viruses in prostate cancer tumors, we employed a DNA microarray-based strategy designed to screen for viruses from all known viral families [20,21]. Total or polyadenylated RNA extracted from tumor tissue was first amplified and fluorescently labeled in a sequence-nonspecific fashion. The amplified and labeled fragments, which contained host as well as potential viral sequences, were then hybridized to a DNA microarray (Virochip, University of California San Francisco, San Francisco, United States) bearing the most conserved sequences of ~950 fully sequenced NCBI reference viral genomes (~11,000 70-mer oligonucleotides).

The Virochip was used to screen RNA samples isolated from prostate tumors of 19 individuals (Figure 1). A positive hybridization signal suggestive of a gammaretrovirus was detected in seven of 11 tumors from patients homozygous for the R462Q RNASEL variant (QQ). In contrast, no virus was detected in three tumors from RQ heterozygotes, and only one of five tumors from RR individuals was positive. Clustering of the microarray oligonucleotide intensities (Figure 1) revealed a similar hybridization pattern in all positive cases. Furthermore, a computational analysis using E-Predict, a recently described algorithm for viral species identification [22], suggested that the same or similar mammalian gammaretrovirus was present in all positive tumors (Table S1). Thus, the Virochip detected the presence of a probable gammaretrovirus in half of the QQ tumor samples and in only one non-QQ sample.

Characterization of XMRV Genome

To further characterize the virus, we recovered its entire genome from one of the tumors (VP35) (Figure 2). To obtain viral clones, we first employed a direct microarray recovery technique described previously [21]. Briefly, amplified nucleic acid from the tumor tissue, which hybridized to viral microarray oligonucleotides, was eluted from two specific spots. The eluted DNA was re-amplified, and plasmid libraries constructed from this material were screened by colony hybridization using the spots' oligonucleotides as probes. The array oligonucleotides used in this case derived from the LTR region of murine type C retrovirus (MTCR) and spleen focus-

In this context, several recent studies have linked germline mutations in RNase L to prostate cancer susceptibility [10–13]. Prostate cancer has a complex etiology influenced by androgens, diet, and other environmental and genetic factors [14]. While sporadic prostate cancer displays an age-related increase in prevalence, familial prostate cancer kindreds often display early-onset disease. Such kindreds, defined by having more than three affected members per family, account for 43% of early onset cases (<55 years old) and 9% of all cases [15]. The genetics of hereditary prostate cancer (HPC) is complex, and several genes have been proposed as susceptibility factors in this syndrome. Interestingly, one of these, *HPC1*, is linked to *RNASEL* [10,11]. Several germline mutations or variants in *HPC1/RNASEL* have been observed in HPC [10–13] (reviewed in [16]), including a common (35% allelic frequency) missense variant of RNase L, in which a G to A transition at nucleotide (nt) position 1385 (G1385A) results in a glutamine instead of arginine at amino acid position 462 (R462Q). Remarkably, a large, controlled sib-pair study implicated the R462Q RNase L variant in up to 13% of unselected prostate cancer cases [11]. One copy of the mutated gene increased the risk of prostate cancer by about 50%, whereas individuals that were homozygous for the mutation had a 2-fold increased risk of prostate cancer. The R462Q RNase L variant had a 3-fold decrease in catalytic activity compared with the wild-type enzyme [9,11]. However, while several case-controlled genetic and epidemiologic studies support the involvement of *RNASEL* (and notably the R462Q variant) in prostate cancer etiology [10–13], others do not [17–19], suggesting that either population differences or environmental factors may modulate the impact of *RNASEL* on prostatic carcinogenesis.

While the antiapoptotic phenotype of RNase L deficiency has dominated previous discussions of its possible linkage to cancer, RNase L is also a key effector of the antiviral action of interferons. This led us to consider the possibility that the putative linkage of RNase L alterations to HPC might reflect enhanced susceptibility to a viral agent. To test this hypothesis, we have examined RNA derived from wild-type and RNase L variant (R462Q) prostate tumors for evidence of

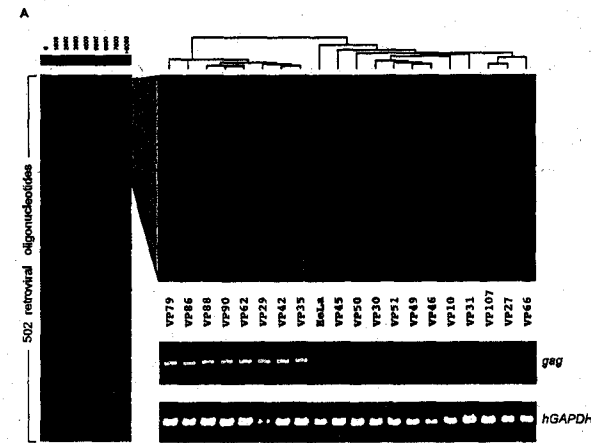


Figure 1. XMRV Detection by DNA Microarrays and RT-PCR

(A) Virochip hybridization patterns obtained for tumor samples from 19 patients. The samples (x-axis) and the 502 retroviral oligonucleotides present on the microarray (y-axis) were clustered using hierarchical clustering. The red color saturation indicates the magnitude of hybridization intensity. (B) Magnified view of a selected cluster containing oligonucleotides with the strongest positive signal. Samples from patients with QQ RNASEL genotype are shown in red, and those from RQ and RR individuals as well as controls are in black. (C) Results of nested RT-PCR specific for XMRV gag gene. Amplified gag PCR fragments along with the corresponding human GAPDH amplification controls were separated by gel electrophoresis using the same lane order as in the microarray cluster. DOI:10.1371/journal.ppat.0020025.g001

forming virus (SFVV) [23]. The largest recovered fragment was 415 nt in length, and had 96% nt identity to the LTR region of MTCR, a MuLV identified in the genome of a mouse myeloma cell line (T. Heinemeyer, unpublished data). These findings established that the virus in question was indeed a gammaretrovirus, and likely a relative of MuLVs. To clone and sequence the rest of the viral genome from sample VP35, we used tumor cDNA to PCR-amplify overlapping segments using primers derived from MTCR; gaps were closed using primers from earlier recovered clones (Figure 2B and Table S2). Using a similar strategy, we have also determined the full sequence of the virus from a second tumor, VP42. Finally, a complete viral genomic sequence from a third tumor case, VP62, was obtained by PCR amplification of two ~4 Kb-long overlapping fragments jointly spanning close to the entire length of the virus (Figure 2B). The three sequenced genomes share >98% nt identity overall and >99% amino acid (aa) identity for predicted open reading frames (ORFs), and thus represent the same virus.

The full genome of the virus (Figures 2 and S1) is 8,185 nt long and is distinct from all known isolates of MuLV. The genome is most similar to the genomes of exogenous MuLVs, DG-75 cloned from a human B-lymphoblastoid cell line [24], and MTCR, with which it shares 94% and 93% overall nt sequence identity, respectively. The genome also shares up to 95% nt identity with several full-length *Mus musculus* endogenous proviruses (Figure 2C). Phylogenetic trees constructed using available mammalian type C retroviral genomes and representative full-length proviral sequences

from the mouse genome (Figures 3 and S2) showed that the newly identified virus is more similar to xenotropic and polytropic than to ecotropic genomes. Based on these findings we propose the provisional name Xenotropic MuLV-related virus (XMRV) for this agent.

Translation of the XMRV genomic sequence using ORF Finder [25] identified two overlapping ORFs coding for the full-length Gag-Pro-Pol and Env polyproteins. No exogenous coding sequences, such as viral oncogenes, could be detected in the XMRV genome. The predicted Gag polyprotein is 536 aa long and is most similar to a xenotropic provirus on *M. musculus* Chromosome 9, with which it shares 97% aa identity (Figure S2A). The Pro-Pol polyprotein is 1,197 aa long and has the highest aa identity with MuLV DG-75 and a xenotropic provirus on *M. musculus* Chromosome 4, 97% and 96%, respectively (Figure S2B). An amber (UAG) stop codon separates the Gag and Pro-Pol coding sequences, analogous to other MuLVs in which a translational read-through is required to generate the full-length Gag-Pro-Pol polyprotein (reviewed in [26]).

Similar to other MuLVs [23,24,27–31], the Env polyprotein of XMRV is in a different reading frame compared with Gag-Pro-Pol. The Env protein sequence is 645 aa long, and has the highest amino acid identity with the Env protein of an infectious MuLV isolated from a human small cell lung cancer line NCI-417 [32] and MuLV New Zealand Black 9-1 xenotropic retrovirus (NZB-9-1) [28]; 95% and 94%, respectively. The XMRV Env protein also shares similarly high identity with several murine xenotropic proviruses

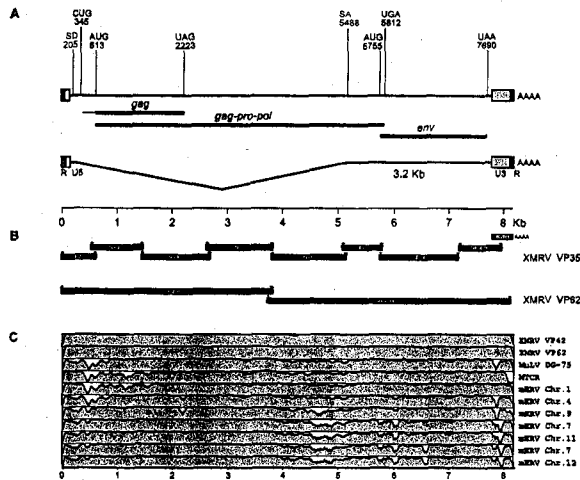


Figure 2. Complete Genome of XMRV
 (A) Schematic map of the 8185 nt XMRV genome. LTR regions (R, U5, U3) are indicated with boxes. Predicted open reading frames encoding Gag, Gag-Pro-Pol, and Env polyproteins are labeled in green. The corresponding start and stop codons (AUG, UAG, UGA, UAA) as well as the alternative Gag start codon (CUG) are shown with their nt positions. Similarly, splice donor (SD) and acceptor (SA) sites are shown and correspond to the spliced 3.2-Kb Env subgenomic RNA (wiggled line).
 (B) Cloning and sequencing of XMRV VP35 and VP62 genomes. Clones obtained by probe recovery from hybridizing microarray oligonucleotides (blue bar) or by PCR from tumor cDNA (black bars) were sequenced. Primers used to amplify individual clones (Table S2) were derived either from the genome of MTCR (black arrows) or from overlapping VP35 clones (blue arrows).
 (C) Genome sequence similarity plots comparing XMRV VP35 with XMRV VP42, XMRV VP62, MuLV DG-75, MTCR, and a set of representative non-ecotropic proviruses (mERVs) (see Materials and Methods). The alignments were made using AVID [81], and plots were generated using mVISTA [82] with the default window size of 100 nt. Y-axis scale for each plot represents percent nt identities from 50% to 100%. Sequences are labeled as xenotropic (X), polytropic (P), modified polytropic (Pm), or ecotropic (E).
 DOI: 10.1371/journal.ppat.0020025.g002

(Figure S2C). Conserved splice donor (AGGTAAG, position 204) and acceptor (CACTTACAG, position 5,479) sites involved in the generation of *env* subgenomic RNAs [33] were found in the same relative locations as in other MuLV genomes. A multiple sequence alignment of XMRV Env and corresponding protein sequences of other representative MuLVs (Figure 4) showed that within three highly variable regions (VR), VRA, VRB, and VRC, known to be important for cellular tropism [34–36], XMRV has the highest aa identity with xenotropic envelopes from MuLVs NZB-9-1, NFS-Th-1 [37], and DG-75. Although unique-to-XMRV aa are present in each of the three VRs, based on the overall similarity to the known xenotropic envelopes, we predict that the cellular receptor for XMRV is XPR1 (SYG1), the recently identified receptor for xenotropic and polytropic MuLVs [38–40].

The long terminal repeat (LTR) of XMRV is 535 nt long and has the highest nt identity with the LTRs from xenotropic MuLVs NFS-Th-1 (96%) and NZB-9-1 (94%). The XMRV LTRs contain known structural and regulatory elements typical of other MuLV LTRs [33,41]. In particular, the CCAAT box, TATAAAA box, and AATAAA polyadenylation signal sequences were found in U3 at their expected locations (Figure S3A). U3 also contains a glucocorticoid response element sequence AGA ACA GAT GGT CCT. Essentially

identical sequences are present in genomes of other MuLVs. These elements have been shown to activate LTR-directed transcription and viral replication *in vitro* in response to various steroids including androgens [42–45]. In addition, presence of an intact glucocorticoid response element is thought to be the determinant of higher susceptibility to FIS-2 MuLV infection in male compared with female NMRI mice [46,47]. Despite these similarities, single nt substitutions unique to XMRV and an insertion of an AG dinucleotide immediately downstream from the TATA box are present in U3 (Figure S3A). Consistent with these findings, a phylogenetic analysis based on U3 sequences from XMRV and from representative xenotropic MuLV provirus groups [48,49] showed that XMRV U3 sequences formed a well-separated cluster most similar to the group containing NFS-Th-1 and NZB-9-1 (Figure S3B).

The 5' *gag* leader of XMRV, defined as the sequence extending from the end of U5 to the ATG start codon of *gag*, consists of a conserved non-coding region of ~200 nt, containing a proline tRNA primer binding site as well as sequences required for viral packaging [50,51] and the initiation of translation [52,53]. The non-coding region is followed by a ~270-nt region extending from the conserved CTG alternative start codon of *gag*. This region represents the

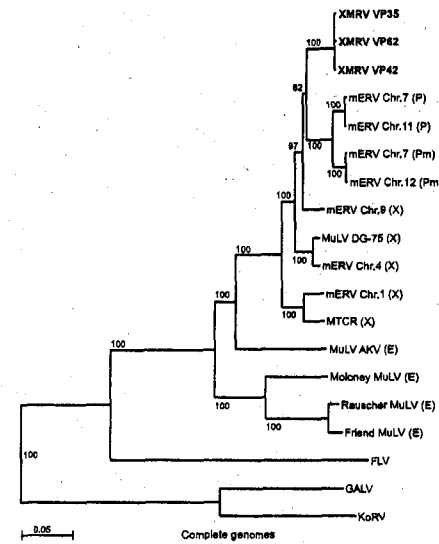


Figure 3. Phylogenetic Analysis of XMRV Based on Complete Genome Sequences
 Complete genomes of XMRV VP35, VP42, and VP62 (red); MTCR; MuLVs DG-75, AKV, Moloney, Friend, and Rauscher; feline leukemia virus (FLV); koala retrovirus (KoRV); gibbon ape leukemia virus (GALV); and a set of representative non-ecotropic proviruses (mERVs) were aligned using ClustalX (see Materials and Methods). An unrooted neighbor-joining tree was generated based on this alignment, excluding gaps and using Kimura's correction for multiple base substitutions. Bootstrap values ($n = 1000$ trials) are indicated as percentages. Sequences are labeled as xenotropic (X), polytropic (P), modified polytropic (Pm), or ecotropic (E).
 DOI: 10.1371/journal.ppat.0020025.g003

most divergent segment of the genome compared with other MuLVs (Figures 5 and 2C). Unlike ecotropic MuLVs, where translation from this codon adds an ~90 aa N-terminal leader peptide in frame with the rest of the Gag protein, thus generating a glycosylated form of Gag [54], XMRV has a stop codon 53 aa residues downstream from the alternative start. Interestingly, both MuLV DG-75 and MTCR *gag* leader sequences are also interrupted by stop codons, and therefore are not expected to produce full-length glyco-Gag. Furthermore, a characteristic 24-nt deletion was present in this region of the XMRV genome, which is not found in any known exogenous MuLV isolate. However, a shorter deletion of nine nt internal to this region is present in the sequences of several non-ecotropic MuLV proviruses found in the sequenced mouse genome (Figure 5). In cell culture, expression of intact glyco-Gag is not essential for viral replication [55,56]. However, lesions in this region have been associated with interesting variations in pathogenetic properties *in vivo* [57–61]. For example, an alteration in ten nt affecting five residues in the N-terminal peptide of glyco-Gag was found to be responsible for a 100-fold difference in the frequency of neuroinvasion observed between CasFrKP and CasFrKP41 MuLV strains [62]. In addition, insertion of an octanucleotide resulting in a stop codon downstream of the CUG start codon prevented severe early hemolytic anemia and prolonged latency of erythroleukemia in mice infected with Friend MuLV [58]. While we do not yet know the pathogenetic significance of the lesions in XMRV glyco-Gag, the high degree of sequence divergence suggests that this region may be under positive selective pressure and therefore may be relevant to the establishment of infection within the human host.

Association of XMRV Infection and R462Q RNASEL Genotype

To further examine the association between presence of the virus and the R462Q (1385G->A) RNASEL genotype, we developed a specific nested RT-PCR assay based on the virus

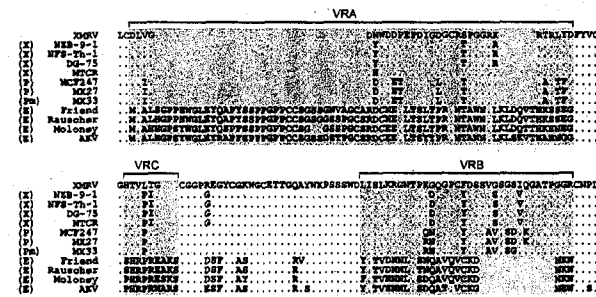


Figure 4. Multiple-Sequence Alignment of Protein Sequences from XMRV and Related MuLVs Spanning SU Glycoprotein VRA, VRB, and VRC, Known to Determine Receptor Specificity
 Env protein sequence from XMRV (identical in VP35, VP42, and VP62; red); MTCR; MuLVs DG-75, NZB-9-1, NFS-Th-1, MCF247, AKV, Moloney, Friend, and Rauscher; and polytropic proviruses MX27 and MX33 [77] were aligned using ClustalX. Sequences are labeled as xenotropic (X), polytropic (P), modified polytropic (Pm), or ecotropic (E). VRs are boxed. Dots denote residues identical to those from XMRV, and deleted residues appear as spaces.
 DOI: 10.1371/journal.ppat.0020025.g004

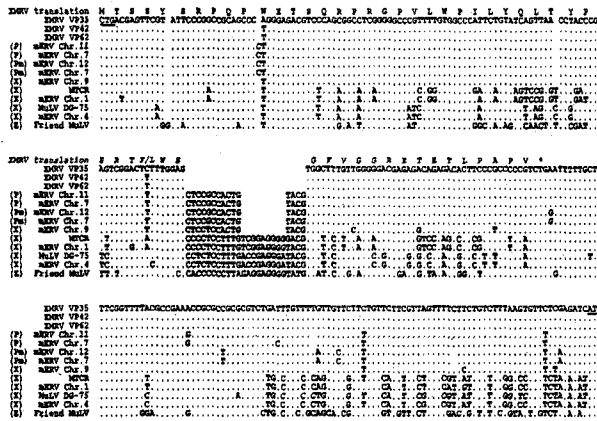


Figure 5. Multiple-Sequence Alignment of 5' gag Leader Nucleotide Sequences from XMRV and Related MuLVs. Sequences extending from the alternative CUG start codon to the AUG start codon (underlined) of gag derived from XMRV VP35, VP42, and VP62 (blue); MTRC, MuLVs DG-75, and Friend; and a set of representative non-ecotropic proviruses (mERVs) were aligned with ClustalX (see Materials and Methods). Predicted amino acid translation corresponding to the VP35 sequence is shown above the alignment (red); asterisk indicates a stop. Sequences are labeled as xenotropic (X), polytropic (P), modified polytropic (Pm), or ecotropic (E). Dots denote nt identical to those from XMRV, and deleted nt appear as spaces. DOI: 10.1371/journal.ppat.0020025.g005

sequence recovered from one of the tumor samples (VP35, see above). The primers in this assay (Figure S1) amplify a 380-nt fragment from the divergent 5' leader and the N-terminal end of gag. The RT-PCR was positive in eight (40%) of 20 examined tumors from homozygous (QQ) individuals. In addition, one tumor from a homozygous wild-type (RR) patient was positive among 52 RR and 14 RQ tumors examined (Figure 1 and Table 1). Interestingly, this case was associated with the highest tumor grade among all XMRV-positive cases (Table S3). PCR specific for the mouse GAPDH gene was negative in all samples (unpublished data), arguing strongly against the possibility that the tumor samples were contaminated with mouse nucleic acid. Collectively, these data demonstrate a strong association between the homozygous (QQ) R462Q RNASEL genotype and presence of the virus, in the tumor tissue ($p < 0.00002$ by two-tail Fisher's exact test).

Table 1. XMRV Screening by gag Nested RT-PCR

PCR	RNASEL Genotype*		Total
	QQ	RQ	
PCR +	8	0	9
PCR -	12	14	77
Total	20	14	86

*RNASEL genotypes are as follows: QQ, homozygous R462Q variant; RQ, heterozygous; RR, homozygous wild-type. DOI: 10.1371/journal.ppat.0020025.t001

XMRV Sequence Diversity in Samples from Different Patients

To examine the degree of XMRV sequence diversity in different patients, we sequenced the amplified fragments from all nine samples, which were positive by the nested gag RT-PCR. The amplified gag fragments were highly similar (Figure 6A) with >98% nt and >98% aa identity to each other. In contrast, the fragments had <89% nt and <95% aa identity with the most related exogenous sequence of MuLV DG-75. Several corresponding endogenous non-ecotropic sequences were more similar to the XMRV fragments, including the xenotropic provirus from *M. musculus* Chromosome 9, which was <98% identical on the nt level. Nevertheless, all XMRV-derived fragments were more similar to each other than they were to any other sequence.

In addition to the gag gene, we also examined the same patient samples for sequence variation in the pol gene. We sequenced PCR fragments obtained with a set of primers targeting a 2500-nt stretch in the pol gene (Figure S1). Similar to the gag fragments, the amplified pol fragments were highly similar (Figure 6B) and had >97% nt and >97% aa identity to each other. In contrast, the fragments had <94% nt and <95% aa identity with the most related sequence, that of MuLV DG-75. Interestingly, XMRV-derived pol sequences were less similar to and approximately equidistant from the examined representative xenotropic and polytropic endogenous sequences.

Close clustering of the sequenced gag and pol fragments (Figure 6) indicates that all microarray and RT-PCR positive cases represent infection with the same virus. On the other hand, the degree of sequence variation in the examined

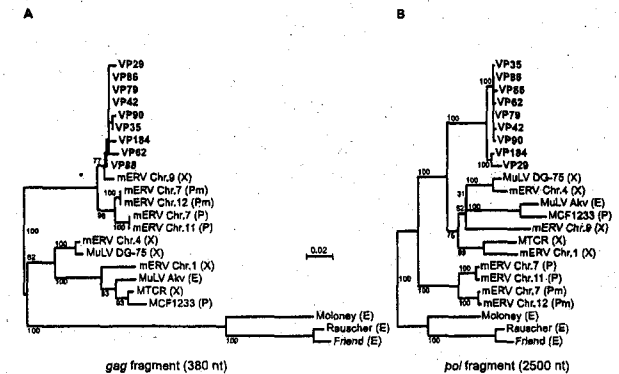


Figure 6. Comparison of XMRV Sequences Derived from Tumor Samples of Different Patients. (A) Phylogenetic tree based on the 380 nt XMRV gag RT-PCR fragment from the nine positive tumor samples (red) and the corresponding sequences from MTRC; MuLVs DG-75, MCF1233, Akv, Moloney, Rauscher and Friend; and a set of representative non-ecotropic proviruses (mERVs). The sequences were aligned using ClustalX, and the corresponding tree was generated using the neighbor-joining method (see Materials and Methods). Bootstrap values ($n = 1000$ trials) are indicated as percentages. Sequences are labeled as xenotropic (X), polytropic (P), modified polytropic (Pm), or ecotropic (E). (B) Phylogenetic tree based on a 2500-nt pol PCR fragment from the 9 XMRV-positive tumor samples. The tree was constructed as described in (A). DOI: 10.1371/journal.ppat.0020025.g006

fragments is higher than that expected from errors introduced during PCR amplification and sequencing. The frequency of nt misincorporation by Taq polymerase has been estimated as $10^{-5} - 10^{-4}$ [63] and references therein), compared with the observed rate of up to 2% in the gag and pol fragments. These findings suggest that the observed XMRV sequence variation is a result of natural sequence diversity, consistent with the virus being independently acquired by the affected patients, and argue against laboratory contamination as a possible source of XMRV.

Detection of XMRV in Tumor-Bearing Prostatic Tissues Using FISH

To localize XMRV within human prostatic tissues, and to measure the frequency of the infected cells, XMRV nucleic acid was visualized using FISH on formalin-fixed prostate tissues. A SpectrumGreen fluorescently labeled FISH probe cocktail spanning all viral genes was prepared using cDNA derived from the XMRV isolate cloned from patient VP35 (Materials and Methods). Distinct FISH-positive cells were observed in the tumors positive for XMRV by RT-PCR (e.g., VP62 and VP88) (Figure 7). To identify cell types associated with the positive FISH signal, the same sections were subsequently stained with hematoxylin and eosin (H&E). Most FISH-positive cells were stromal fibroblasts (Figure 8A), including those undergoing cell division (Figure 8B). In addition, occasional infected hematopoietic cells were also seen (Figure 8C). XMRV FISH with concurrent immunostaining for cytokeratin AE1/AE3 to achieve specific labeling of epithelial cells [64] showed no XMRV-infected cells that also had the epithelium-specific staining, confirming their non-epithelial origin (Figure 8C). While the XMRV nucleic acid was usually present within nuclei (Video S1), suggesting integrated proviral DNA, some cells showed cytoplasmic

staining adjacent to the nucleus, suggestive of viral mRNA and/or pre-integration complexes in non-dividing cells (Figure 8A).

We also used FISH to obtain a minimal estimate of the frequency of XMRV-infected prostatic cells. For this purpose we employed a tissue microarray containing duplicates of 14 different prostate cancer tissue specimens (Table 2). FISH with DNA probes derived from XMRV VP35 showed five to ten XMRV/FISH-positive cells (about 1% of prostate cells observed) in each of five homozygous (QQ) cases (VP29, 31, 42, 62, and 88). Patient sample LP79, also a QQ case, contained two positive cells (0.4% of total cells examined). All of the XMRV/FISH-positive cells observed were stromal cells. In contrast, three RR tissue samples and two RQ tissue samples showed one or no (<0.15%) FISH-positive cells. Two of the QQ cases, VP35 and VP90, positive by gag RT-PCR, showed only one FISH-positive cell each (Table 2). Conversely, one case, VP31, was FISH-positive, but gag-RT-PCR negative. As expected, Chromosome 1-specific probes used as a positive control specifically labeled nearly every cell from the examined case VP88, whereas a KSHV-specific probe used as a negative control did not label any cells in sections from cases VP88 and VP51, but did efficiently label 293T cells transfected with KSHV DNA (unpublished data). Thus, consistent with the microarray and RT-PCR data, detection of XMRV by FISH was associated primarily with QQ cases. In addition, in samples where XMRV was detected, all positive cells were stromal and did not account for more than 1% of all prostatic cells. Finally, differences in the numbers of XMRV-positive cells detected in the different samples could be due to heterogeneity in virus copy numbers between different patients and/or specific regions of the prostate sampled.

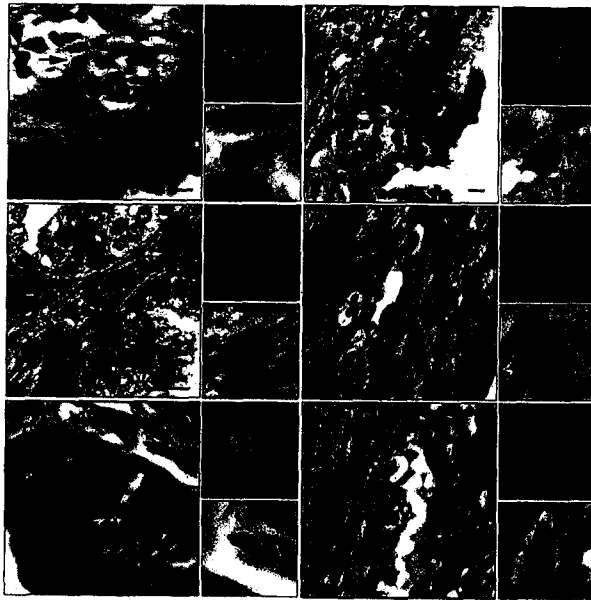


Figure 7. Detection of XMRV Nucleic Acid in Prostatic Tissues Using FISH
Prostatic tumor tissue sections from QQ cases VP62 (A–C) and VP88 (D–F) were analyzed by FISH using DNA probes (green) derived from XMRV VP35 (top right enlargements). Nuclei were counterstained with DAPI. The same sections were then visualized by H&E staining (left panels). Scale bars are 10 μm. Arrows indicate FISH positive cells, and their enlarged images are shown in the bottom right panels.
DOI: 10.1371/journal.ppat.0020025.g007

Detection of XMRV in Tumor-Bearing Prostatic Tissues Using IHC

To identify cells expressing XMRV proteins, we assayed for the presence of Gag protein using a monoclonal antibody against (SFFV); this antibody is reactive against Gag proteins from a wide range of different ecotropic, polytropic, and xenotropic MuLV strains [65]. Using this antibody, positive signal by IHC was observed in prostatic tissues of XMRV-positive cases VP62 and VP88, both QQ (Figure 9). An enhanced alkaline phosphatase red detection method allowed Gag detection in the same cells with both fluorescence (Figure 9A–9D, left) and bright field (Figure 9A–9D, middle) microscopy. The Gag-expressing cells were observed in prostatic stromal cells with a distribution and frequency similar to that detected by FISH (Figure 9 and unpublished data). In contrast, no Gag-positive cells were observed in VP51 prostatic tissue, which is of RR genotype (Figure 9E).

Discussion

The results presented here identify XMRV infection in prostate tissue from approximately 40% of patients with prostate cancer who are homozygous for the R462Q variant (QQ) of RNase L, as judged by both hybridization to the

Virochip microarray and by RT-PCR with XMRV-specific primers. Parallel RT-PCR studies of prostate tumors from wild-type (RR) and heterozygous (RQ) patients revealed evidence of XMRV in only one of 66 samples, clearly demonstrating that human XMRV infection is strongly linked to decrements in RNase L activity. This result supports the view that the R462Q RNase L variant leads to a subtle defect in innate (IFN-dependent) antiviral immunity.

As its name indicates, XMRV is closely related to xenotropic murine leukemia viruses (MuLVs). Unlike ecotropic MuLVs, such as the canonical Moloney MuLV, which grow only in rodent cells in culture, xenotropic MuLVs can grow in non-rodent cells in culture but not in rodent cell lines. Xenotropic viruses have been isolated from many inbred as well as wild mouse strains. Studies of the distribution of non-ecotropic sequences in different mouse strains show that the diversity of xenotropic proviral sequences in wild mice is greater than that found in the inbred laboratory strains [49,66]. This finding led to the conclusion that these endogenous elements were independently and relatively recently acquired by different mouse species as a result of infection rather than inheritance [49]. Unlike ecotropic MuLVs, which can only recognize a receptor (CAT-1) specific to mouse and rat species [67–69], xenotropic

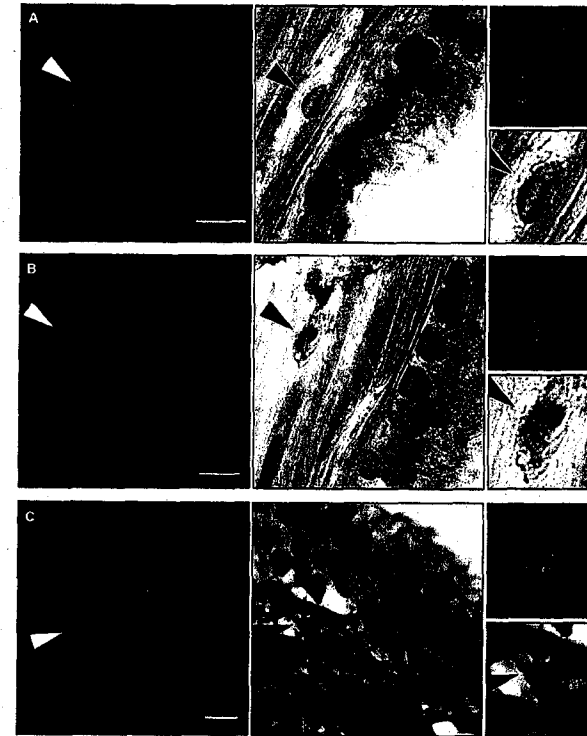


Figure 8. Characterization of XMRV-Infected Prostatic Cells by FISH and FISH/Immunofluorescence
Using a tissue microarray, prostatic tumor tissue sections from QQ case VP62 were analyzed by FISH (green) using DNA probes derived from XMRV VP35 (left panels). Nuclei were counterstained with DAPI. The same sections were then visualized by H&E staining (middle panels). Arrows indicate FISH-positive cells, and their enlarged FISH and H&E images are shown in the top right and bottom right panels, respectively. Scale bars are 10 μm.
(A) A stromal fibroblast.
(B) A dividing stromal cell.
(C) A stromal hematopoietic cell. The section was concomitantly stained for XMRV by FISH (green) and cytokeratin AE1/AE3 by immunofluorescence (red).
DOI: 10.1371/journal.ppat.0020025.g008

viruses recognize a protein known as XPR1 or SYG1. XPR1 is expressed in all higher vertebrates, including mice, but polymorphisms in the murine gene render it unable to mediate xenotropic MuLV entry [38–40]. Thus, xenotropic MuLVs have a potential to infect a wide variety of mammalian species, including humans.

Xenotropic MuLVs have occasionally been detected in cultured human cell lines. For example, MuLV DG-75 was cloned from a human B-lymphoblastoid cell line [24], and an infectious xenotropic MuLV was detected in a human small cell lung cancer line NCI-417 [32]. Although laboratory contamination, either in culture or during passage of cell lines in nude mice, cannot be ruled out as a possible source in these cases, such contamination cannot explain our results.

The evidence for this is as follows: (i) XMRV was detected in primary human tissues; (ii) no murine sequences (e.g., GAPDH) could be detected in our materials by PCR; (iii) infection was predominantly restricted to human samples with the QQ RNASEL genotype; (iv) polymorphisms were found in the XMRV clones recovered from different patients consistent with independent acquisition of the virus by these individuals; and (v) viral nucleic acids and antigens could be detected in infected QQ prostate tissue by FISH and IHC, respectively. Taken together, the above evidence argues strongly against laboratory contamination with virus or cloned DNA material as the source of XMRV infection in the analyzed samples. To our knowledge, this report represents the first published examples of authentic infection